ELSEVIER

Materials Science and Engineering B94 (2002) 196–201

MATERIALS SCIENCE & ENGINEERING B

www.elsevier.com/locate/mseb

Comparison of strain relaxation in epitaxial $Si_{0.3}Ge_{0.7}$ films grown on Si(001) and Ge(001)

B.G. Demczyk [a,1], V.M. Naik [b], S. Hameed [c], R. Naik [c,*]

[a] Air Force Research Laboratory, SNHX, Hanscom AFB, MA 01731, USA
[b] Department of Natural Sciences, The University of Michigan-Dearborn, Dearborn, MI 48128, USA
[c] Department of Physics and Astronomy, Wayne State University, Detroit, MI 48202, USA

Received 19 December 2001; accepted 12 February 2002

Abstract

Epitaxial $Si_{1-x}Ge_x$ films of thickness ~200 nm have been grown on Si(100) and Ge(100) substrates using chemical vapor deposition. Both X-ray diffraction and Raman studies show that the films are Ge rich ($x = 0.7$) with no residual strain. Cross-sectional transmission electron microscopy studies have been used to demonstrate that the films relax by different mechanisms leading to different surface morphology and interface structure. Films in tension (SiGe/Ge) were seen to relax through the creation of misfit dislocations, whereas those in compression (SiGe/Si) formed islands without dislocations. Consideration of the misfit dislocation formation mechanism in these materials has been used to explain this behavior phenomenologically. © 2002 Elsevier Science B.V. All rights reserved.

Keywords: SiGe alloy films; Raman spectroscopy; Strain relaxation; Epitaxy; Dislocations; Transmission electron microscopy

1. Introduction

The growth of semiconductor heteroepitaxial layers is assuming ever greater importance due to the demands of modern electronic-device fabrication. The SiGe system is of particular interest due to its lower cost and inherent compatibility with Si lithographic technology. Due to the complete miscibility of Si and Ge [1], alloys of any desired composition can, in principle, be synthesized, giving rise to a number of interesting high speed and optoelectronics applications [2]. In particular, materials with bandgaps in the 1.3–1.55 μm range, corresponding to Ge concentrations of 25% or more are of interest in optical communication and in infrared detection [3]. Due to the relatively large (up to ~4%) lattice mismatch between Si and Ge, growth of individual SiGe layers of appreciable Ge concentration will nominally be limited to below the a critical thickness [4,5], beyond which interfacial misfit defects will be introduced. These misfit dislocations differ from dislocations in the usual sense in that they decrease the total energy of the system, and, thus, are thermodynamically favored. Both $\alpha = 60$ and 90° dislocations (α is the angle between the dislocation line and the Burger's vector, **b**) have been observed in the SiGe system [6]. Although 90° dislocations reduce the strain more efficiently than 60° ones (nb versus nb/2 for an array of n dislocations), the latter are generally formed preferentially in all but the thinnest strained layers due to their lower energy of self formation. These defects degrade device performance by increasing dark currents and noise. A large body of both experimental and theoretical work has been devoted to this topic [6,7], and a number of design concepts have emerged to produce low dislocation density epitaxial layers, involving the use of compositional grading [8,9].

Aside from the well established problems associated with misfit dislocation formation in SiGe alloy growth on Si, an additional phenomenon, three-dimensional island formation, has attracted interest in recent years. These structures form as a result of stress-enhanced diffusion [10] of Ge in response to high strain (i.e. high Ge content) and/or high temperature depositions. The

* Corresponding author. Tel.: +1-313-577-2104; fax: +1-313-577-3932.
E-mail address: naik@physics.wayne.edu (R. Naik).
[1] Present address: MMC Technology, 2000 Fortune Drive, MS 15161, San Jose, CA 95131, USA.

0921-5107/02/$ - see front matter © 2002 Elsevier Science B.V. All rights reserved.
PII: S0921-5107(02)00084-3

equilibrium surface morphology that develops is a minimum energy configuration, as the strain energy relieved by lattice relaxation is offset by the additional surface energy associated with the 'wavy' interfaces. Although these asperities can, in principle act as sources for misfit dislocations [11], other studies [12] have found them to be largely dislocation-free. This suggests that they provide an alternate pathway for strain energy reduction. Since this morphology is detrimental to the fabrication of multilayer structures proposed in various device applications, it is of paramount importance that a firm understanding of conditions under which such morphologies evolve be understood. Such three dimensional arrays are also of interest in their own right, as three-dimensional quantum confinement structures, with enhanced (with respect to two-dimensional quantum wires) blue shifted luminescence are observed [13]. These quantum 'dots', comprised of clusters of a few thousand atoms, confine charge carriers in three dimensions. It is thus of considerable interest to extend studies of these alloy compositions into the regimes of high compressive (i.e. high Ge content layers on Si) and tensile (through deposition onto single crystal Ge substrates) strains.

In this work we report X-ray diffraction (XRD), Raman spectroscopy, atomic force microscopy (AFM) and cross-sectional transmission electron microscopy (TEM) studies on epitaxial Si_{1-x} Ge_x ($x = 0.7$) films grown on Si(100) and Ge(100) substrates to elucidate the degree to which and how strain is relieved and its influence on the resulting surface morphology. Films in tension seem to relax through the creation of misfit dislocations, whereas those in compression form islands. This observed behavior is explained phenomenologically by considering the mechanism of formation of misfit dislocations in these materials

2. Experimental procedure

Epitaxial films of $Si_{1-x}Ge_x$ were grown at the Air Force Research Laboratory, (AFRL) on single crystal Si (001) and Ge (001) substrates by ultrahigh vacuum chemical vapor deposition at 600 °C to a thickness of 200 nm. The growth rate was less than 0.1 nm s^{-1}. All substrates were preoxidized in ozone, followed by oxide removal via an HF dip, (10% by volume) to provide hydrogen-terminated surfaces immediately prior to film growth. XRD $\theta - 2\theta$ and rocking curve scans were performed with a Rigaku powder diffractometer using Cu-Kα radiation. Raman spectra were measured in the back scattering geometry, using a Spex 1404 double monochomater equipped with photon counting electronics. The 514.5 nm line from an argon laser was used to excite the Raman spectra. Incident laser power of ~100 mW was focused to a spot on the sample. The spectral band pass was ~2.5 cm^{-1} at 514.5 nm, and the step resolution used was 0.5 cm^{-1}. The surface morphology of the films was examined with a Digital Instruments Nanoscope III AFM, operating in the tapping mode. For TEM studies, section samples were prepared by bonding two films face to face, mechanical thinning and ion beam thinning. Conventional transmission (100 kV) electron microscopy (TEM), and ex-situ reflection high energy (60 kV) electron diffraction (RHEED) results were obtained utilizing facilities at AFRL, while high resolution (200 kV) electron microscopy (HREM) was conducted at the MIT Lincoln Laboratory.

3. Results and discussion

Both XRD and Raman data were utilized to determine the composition and residual strains in epitaxial $Si_{1-x}Ge_x$ films grown on Si(001) and Ge(001) substrates. Fig. 1(a) and (b) display the sharp (004) peak of $Si_{1-x}Ge_x$ (shifted with respect to the substrate peaks), along with the rocking curve scans shown as inset. XRD data clearly indicate a well oriented $\langle 001 \rangle$ growth of the films. Fig. 2(a) and (b) show their corresponding Raman spectra with strong peaks of Ge–Ge and Ge–Si optical phonon modes. For partially strained alloys, the Raman shift of the Ge–Ge, Ge–Si and Si–Si optical phonon

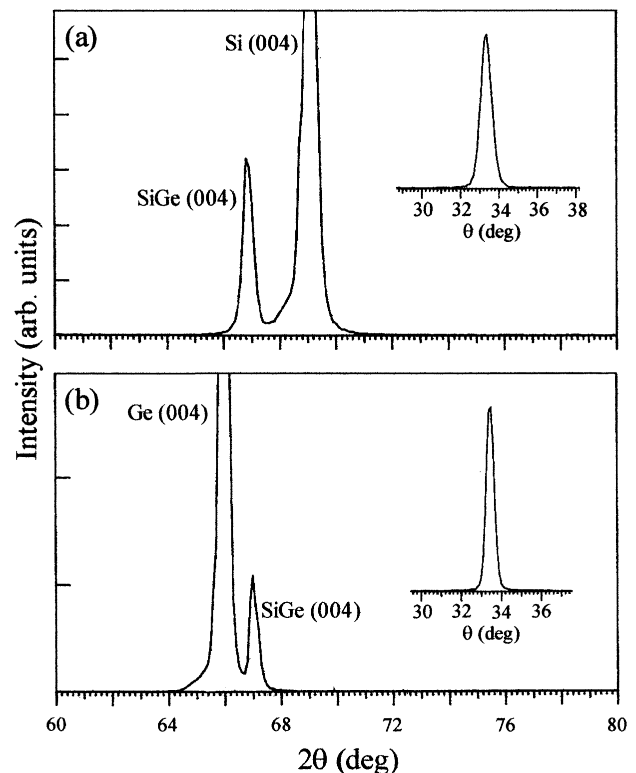

Fig. 1. X-ray diffraction pattern of SiGe alloy on (a) Si (001), (b) Ge (001) substrate. The insets shown are the rocking curves of the Si_{1-x} Ge_x (004) peak.

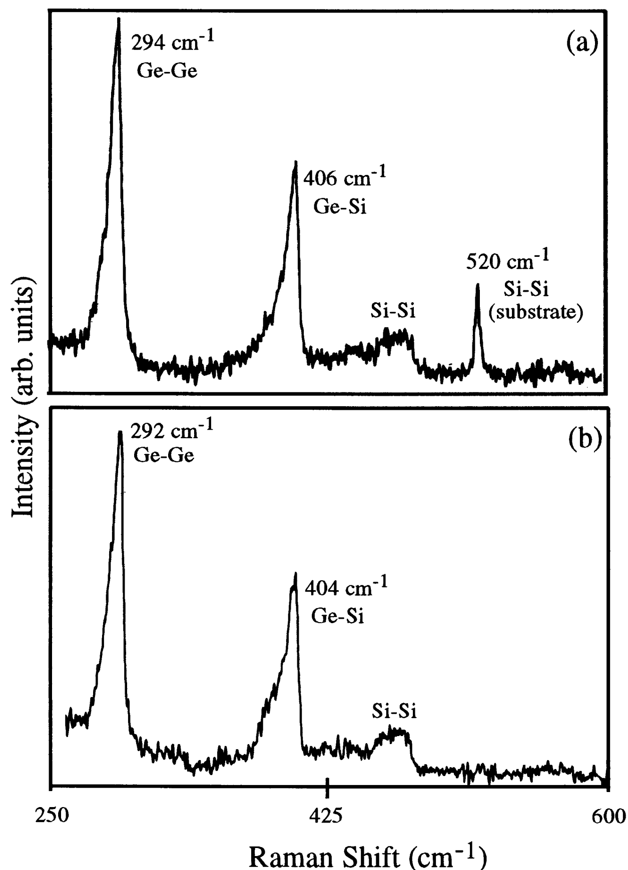

Fig. 2. Raman spectrum of SiGe alloy on (a) Si (001), (b) Ge (001) substrate.

modes are given by [14]:

$$\omega_{\mathrm{Ge/Ge}} = 300 - 20x - 17x\Gamma \quad (1a)$$

$$\omega_{\mathrm{Ge-Si}} = 390 + 55x - 17x\Gamma \quad (1b)$$

$$\omega_{\mathrm{Si-Si}} = 456 + 66x - 28x\Gamma \quad (1c)$$

Here, $\Gamma(=(\delta l/l)(1/0.0417))$ is the strain ratio, $\delta l/l$ is the parallel strain and x the Ge concentration. Using the experimentally observed Raman shifts for the Ge–Ge and Ge–Si peaks (Si–Si peaks are too broad), we obtain values of $x \sim 0.69$ (films are Ge-rich) and $\varepsilon_{||}$ of -0.00135 and $+0.00058$ for SiGe/Si and SiGe/Ge. These low values of $\varepsilon_{||}$ indicate that, on average, the epitaxial layers are nearly fully relaxed. Utilizing these results, the lattice parameter of the alloy film is calculated from the equation $a(x) = 0.5431 + 0.02x + 0.002x^2$ [15], yielding $a = 0.5581$ nm which compares well with the XRD data. Hence, lattice misfit, δ $(=(a_{\mathrm{epi}} - a_{\mathrm{sub}})/a_{\mathrm{sub}})$ is $+0.029$ and -0.013 for the SiGe/Si and SiGe/Ge.

The surface morphology of the films was studied using AFM (Fig. 3a and 3b). In both cases, an islanded morphology is evident with somewhat larger islands in SiGe/Ge. Since the surface energy of the SiGe lies between that of Ge (lowest) and Si (highest), one would expect a complete coverage of Si by the SiGe film and an incomplete coverage of Ge by the same. However, the development of similar resultant morphologies in both films is worth noticing. Perhaps the stress relieving mechanisms in these two cases (film in compression for SiGe/Si and in tension for SiGe/Ge) influence the initial morphology of the epitaxial layers over and above what surface energy considerations would dictate.

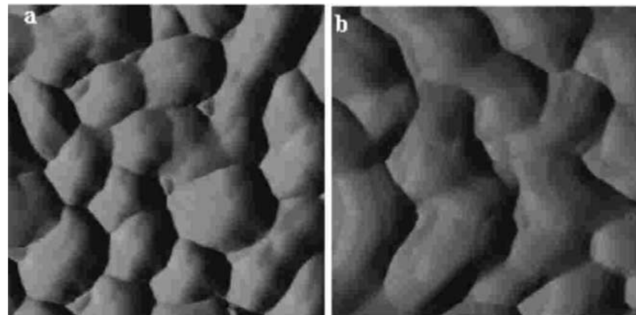

Fig. 3. Atomic force micrograph of SiGe alloy on (a) Si (001), (b) Ge (001) substrate. Scan size is 2×2 μm.

To investigate the strain relaxation mechanism in detail, cross-sectional TEM was undertaken. Fig. 4(a) and (b) are cross sectional TEM views of the SiGe/Si and SiGe/Ge interfaces. The SiGe/Si film grows from the outset with a discrete, faceted island morphology, whereas SiGe/Ge initially forms a planar layer and only roughens after attaining a thickness of ~ 100 nm.

Strain relaxation in strained films would normally be expected to involve the nucleation and movement of dislocations. These misfit dislocations are thought to form either by motion of a threading dislocation from the substrate or nucleation and propagation of dislocation half loops at and from the surface. The biaxial stresses in the film exert forces on the threading dislocation segment and cause it to move in the slip plane. The portion of the dislocation that resides in the substrate remains stationary because the forces on it are much smaller and oppose each other. Thus, the threading dislocation in the film bends over as it moves and

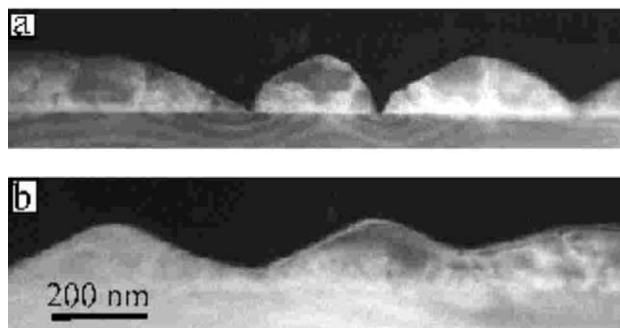

Fig. 4. Cross sectional TEM image of 200 nm thick SiGe alloy on (a) Si (001), (b) Ge (001) substrate. Beam direction is along ⟨110⟩ of the substrate.

eventually leaves a misfit dislocation in its wake. Continued movement of the threading dislocation extends the length of the misfit dislocation. Alternatively, dislocation half loops can be nucleated at the free surface of the growing film and eventually lead to the formation of misfit dislocations at the interface as the two ends of the half loop move in opposite directions (similar to a Frank–Read mechanism). People and Bean [16] have argued that the bending of existing threading dislocations is unlikely to serve as a significant source of misfit dislocations for small misfits and that the nucleation of stable dislocation half loops is unlikely unless the misfit is large. The paucity of existing threading dislocations in semiconductor substrates, however, leaves the half loop nucleation mechanism as the most plausible.

In these diamond cubic materials, the dislocations are of the 60° mixed type, with $b = 1/2\{01\bar{1}\}\langle 111\rangle$, (Burgers vector makes an angle of $\sim 45°$ with (001)). Now, to both lower their total energy ($\sim b^2$, according to Frank's rule) and to reduce their core width (thus lowering the Peierls–Nabarro stress), these 60° perfect dislocations will dissociate into leading and trailing partial dislocations, each with Burgers vector of type $1/6\langle 112\rangle$. Consider now the slip mechanism on (111) under the action of a tensile stress (as per Fig. 5). As shown, the 60° perfect dislocation has dissociated into a leading 90° (i.e. b is normal to the dislocation line of the original perfect dislocation) and a trailing 30° partial. Now, the imposed stress will be resolved on the slip plane in the slip direction, say τ. Under the action of the tensile stress, the force on the leading partial will then be $\tau b \cos 30°$ ($= 0.866\ \tau b$), while that on the trailing partial is $\tau b \tan 30°$ ($= 0.577\ \tau b$), b in each case being of the same magnitude (0.408 nm). Therefore, the first partial will nucleate rapidly, but the second will be delayed (due to the smaller force on it), resulting in the formation of an extended pair (with a stacking fault between them). In the case of compressive stress (arrows reversed in Fig. 5), the nucleation of the now leading 30° partial will be delayed, due to the smaller resolved stress along it. Once the leading partial does nucleate, however, it will be followed rapidly by the trailing 90° partial. Therefore, the pair will be barely extended and will move in lock-step. Maree et al. [17] have considered the energy required to nucleate a dislocation half loop for both tensile and compressive strain. When factors such as the energy released in forming the loop and the stacking fault are added and the energy lost through movement of the partials are taken into account, it is found that the net energy required for nucleation of a half loop in the case of tension is less than in compression, and can be lower than that derived without taking these additional energy terms into account. Consequently, misfit dislocation formation via the half-loop mechanism is favored in the case of tension. The influence of the sign of the misfit strain on the relaxation mechanism generally has not been addressed heretofore in these materials.

Close examination of the region between the islands in Fig. 4(a) reveals the presence of strain contrast in the substrate, with maximum strain near the island center. No such features are present in the Ge substrate in Fig. 4(b). However, a considerable density of dislocations is evident along the interface. In this case, the film is in tension and strain is accommodated through the formation of misfit dislocations of spacing, S, on the order of b/δ, where b is the Burgers vector and δ, the misfit. Taking $b = 0.4$ nm and $\delta = 0.013$, as above, we obtain $S \sim 30$ nm, or approximately 90 {111} planes. High-resolution electron microscopy images taken across the interface under an island reveal considerable strain contrast across the interface in the SiGe/Si case (Fig.

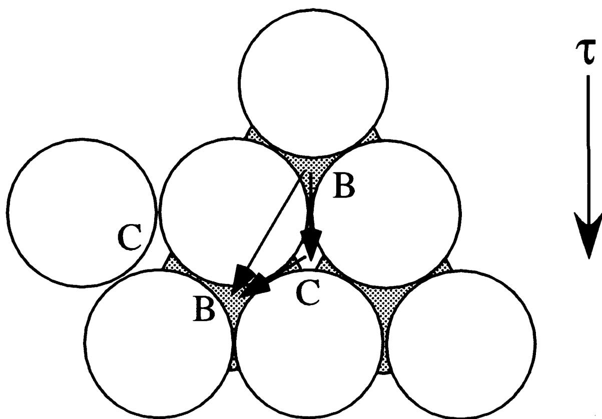

Fig. 5. Schematic of slip mechanism of 60° dislocation on (111)(adapted from [17]).

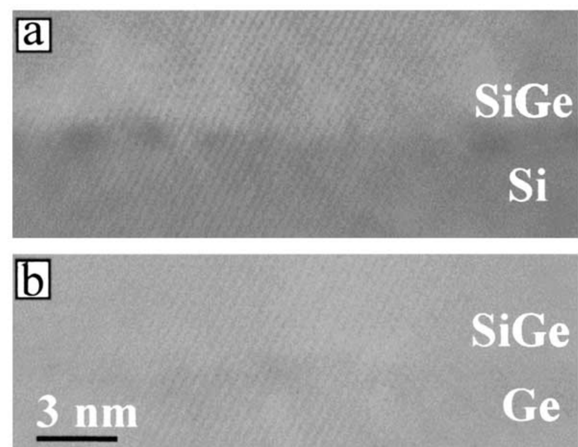

Fig. 6. High resolution cross sectional transmission electron micrograph of SiGe alloy on (a) Si (001), (b) Ge (001) substrate. Beam direction is along ⟨110⟩ of the substrate.

6(a)). No such contrast is seen across the SiGe/Ge interface (Fig. 6(b)). This is the region between dislocations and is strain-free (well lattice matched). The film/substrate mismatch measured directly across the interface by HREM was 0.041 and −0.012 for SiGe/Si and SiGe/Ge. The near-surface (within 10 nm of the surface) mismatch of SiGe/Si, relative to bulk Si was determined by RHEED to be 0.017, while that of SiGe/Ge, relative to bulk Ge, was −0.015. These results bracket those derived from Raman spectroscopy and XRD, which represent a volume-average. The SiGe/Si results suggest that stress-driven diffusion [10] of Ge along the island surface towards the substrate has occurred. This would account for the lack of strain contrast in the region between the islands in Fig. 4(a). In SiGe/Ge, we do not observe such effects, since all the misfit strain is accommodated by misfit dislocations. Curiously enough, however, the film develops a three-dimensional morphology and at an apparent (surface energy) cost, even though it is (by then) strain-free. Examination of Fig. 4(b), however, reveals that these islands contain large facets of nearly $\langle 111 \rangle$ orientation, which is a lower energy surface than the original $\langle 001 \rangle$. Therefore, the surface energy is, in fact, reduced.

Consequently, absent any film-substrate misfit strain, systems tend to maximize (111) surface area at the expense of other orientations, such as (001). Xie et al. [18] have observed roughening in $Si_{0.5}Ge_{0.5}$ films grown on a compositionally-graded SiGe layer (on Si(001)) under compressive stress and no roughening in films deposited in tension. They attributed this behavior to a lowering of monatomic and diatomic step energies induced by the compressive stress. Tersoff [19] has since argued that step energetics play a relatively minor role in the roughening of SiGe(001) films, which, instead take the form of (105) faceting [20,21]. He further points out that the surface stress can change with the sign of the misfit, since by definition the surface stress, itself, is the change of the surface energy with strain. It should be noted that the multilayer system described by Xie et al. [18] differs from the present case in that the compositionally-graded SiGe layer is elastically softer than either Ge or Si substrates alone. This, according to the Asaro and Tiller formalism [22] would induce enhanced roughening when compared with films deposited on bulk substrates. Guyer and Voorhees [23,24] have incorporated film formation kinetics into their theoretical model to derive morphological stability maps, which show surface perturbation wavelengths that differ with the sign of the film/substrate misfit. Their analysis draws heavily on the premise that local compositional inhomogeneities in the growing film drive the morphological instabilities. In the present work, the complementary pairs, SiGe/Ge (planar) and SiGe/Si (islanded), provide evidence that the sign of the misfit strain can affect profoundly the resultant film morphology. Comparison of experimental measurements of both interplanar spacings near the surface and film-substrate misfits across the interface confirms that the lattice parameter is increased from that of the substrate to that of the bulk deposit within these islands.

4. Conclusions

A study of the surface morphology and interface structure of Ge-rich Si–Ge films, grown by ultrahigh vacuum chemical vapor deposition on Si (001) and Ge (001) substrates has revealed two independent, but competing factors that combine to determine the resulting film morphology. When misfit strain is present, the systems seek to relieve it through the formation of misfit dislocations. Although it is to be expected that misfit dislocation formation is facilitated by large strains, it was found that the sign of the strain is equally important. In particular, compressively strained films (SiGe/Si) tend to form surface asperities to relax the misfit strain without forming dislocations, while reducing the surface free energy. On the other hand, the films in tension (SiGe/Ge) relieve their strain by the formation of dislocations initially and then forming three dimensional $\langle 111 \rangle$ facets to lower the surface free energy.

Acknowledgements

The authors wish to thank Dr Leanne Henry, now at the US Military Academy and Kenneth Vaccaro of AFRL for their assistance with epitaxial growth and Paul Nitishin of the MIT Lincoln Laboratory for facilitating the high resolution work. Financial support was provided by the US Air Force Palace Knight program.

References

[1] S. Freyan, D.M. Wood, A. Zunger, Phys. Rev. B. 37 (1988) 6893.
[2] E. Kaspar, J. Cryst. Grwth. 150 (1995) 921.
[3] D.P. Pearsal, H. Temkin, J.C. Bean, IEEE Elec. Dev. Lett. EDL-7 (5) (1986) 330.
[4] J.H Van der Merwe, J. Appl. Phys. 34 (1962) 123.
[5] J.W. Mathews, A.E. Blakeslee, J. Cryst. Gwth. 27 (1974) 118.
[6] J. Narayan, S. Sharan, Mat. Sci. Eng. B 10 (1991) 261.
[7] P.M. Mooney, F.K. LeGoues, J. Tersoff, J.O. Chu, J. Appl. Phys. 75 (1994) 3968.
[8] E.A. Fitzgerald, Y.H. Xie, D. Monroe, P.J. Silverman, J.M. Kuo, A.R. Kortan, F.A. Thiel, B.J. Weir, J. Vac. Sci. Technol. B 10 (1807) 1992.
[9] P.M. Mooney, J.L. Jordan-Suret, J.O. Chu, F.K. LeGoues, Appl. Phys. Lett. 66 (1995) 3642.
[10] J. Tersoff, F.K. LeGoues, Phys. Rev. Lett. 75 (1994) 3570.
[11] F.K. LeGoues, MRS Bull. 21 (4) (1995) 39.

[12] A.G. Cullis, D.J. Robbins, A.J. Padduck, P.W. Smith, J. Cryst. Growth 123 (1992) 333.
[13] R. Apez, R. Loo, L. Vescan, A. Hartmann, U. Zastrans, A. Leuter, T. Schapes, H. Lutn, Solid State Comm. 37 (1994) 957.
[14] D.S. Gu, L. Qin, R. Zhang, X. Zhu, Y. Zheng, Appl. Phys. Lett. 62 (1996) 387.
[15] J. Lockwood, J.-M. Baribeau, Phys. Rev. B 45 (1992) 8565.
[16] R. People, J.C. Bean, Appl. Phys. Lett. 47 (1985) 322.
[17] P.M. Maree, J.C. Barbour, J.F. Van der Veen, K.L. Kavanagh, C.W.T. Bulle-Lieuwma, M.P.A. Viegers, J. Appl. Phys. 62 (1987) 4413.
[18] Y.H. Xie, G.H. Gilmer, C. Roland, P.J. Silverman, S.K. Burrato, J.Y. Cheng, E.A. Fitzgerald, A.R. Kortan, S. Schuppler, M.A. Marcus, P.H. Citrin, Phys. Rev. Lett. 73 (1994) 3006.
[19] J. Tersoff, Phys. Rev. Lett. 74 (1995) 4962.
[20] Y.M. Mo, D.E. Savage, B.S. Swartzentruber, M.G. Lagally, Phys. Rev. Lett. 65 (1990) 1020.
[21] M.A. Lutz, R.M. Feenstra, P.M. Mooney, J. Tersoff, J.O. Chu, Surf. Sci. Lett. 316 (1994) L1075.
[22] R.J. Asaro, W.A. Tiller, Metall.Trans. 3 (1972) 1789.
[23] J.E. Guyer, P.W. Voorhees, Phys. Rev. B 54 (16) (1996) 11710.
[24] J.E. Guyer, P.W. Voorhees, Phys. Rev. Lett. 74 (20) (1995) 4031.